Ecological Indicators 84 (2018) 738–747

Contents lists available at ScienceDirect

Ecological Indicators

journal homepage: www.elsevier.com/locate/ecolind

Research paper

Evaluating the timing of the start of the Anthropocene from Northeast China: Applications of stratigraphic indicators

Hanxiang Liu[a,b], Chuanyu Gao[a,*], Chunfeng Wei[a], Chunling Wang[c], Xiaofei Yu[a], Guoping Wang[a,*]

[a] Key Laboratory of Wetland Ecology and Environment, Northeast Institute of Geography and Agroecology, Chinese Academy of Sciences, Changchun, 130102, China
[b] University of Chinese Academy of Sciences, Beijing, 100049, China
[c] College of Urban and Rural Construction, ShanXi Agricultural University, Jinzhong, 030801, China

ARTICLE INFO

Keywords:
Sedimentological parameters
Geochemistry
Biological indicator
Historical document records
Sanjiang plain

ABSTRACT

The Earth can be described as having entered a new human-dominated geological epoch that is known as the "Anthropocene", and determining the timing of the start of the Anthropocene has become important. Here, we combined sedimentological parameters (sedimentation rate and mean grain size), geochemical indicators (heavy metal enrichment factors, black carbon fluxes and polycyclic aromatic hydrocarbons concentrations) and a biological indicator (plant macrofossils) in wetland sediment records to assess the start of the Anthropocene. The analysis of five wetlands on the Sanjiang Plain, Northeast China, showed that the major component scores of sedimentological parameters and geochemical features based on principal component analyses had obvious increasing trends after the 1950s. Structural change tests were applied to the plant macrofossil data of one typical peatland to detect the breakpoint of the wetland ecosystem, and the dominant species of the plant community changed from *Carex lasiocarpa* to *Salix myrtilloides* during this period due to intensive human activities and drainage in this region. We can divide the history of anthropogenic activities into five periods among the three phases of exploitations that occurred in the Sanjiang Plain, Northeast China, based on our results and historical document records; the anthropogenic activities increased significantly starting in the New China period. It is suggested that the 1950s can be treated as the start of the Anthropocene on the Sanjiang Plain, Northeast China. Similar studies of stratigraphic indicators that provide estimates of historical human activities in other regions could contribute to the global definition of the Anthropocene.

1. Introduction

Global environment issues, such as climate change, land and atmosphere pollution, and biodiversity loss, are raising concerns about the viability of human civilization. Human activities have become so profound and pervasive that the Anthropocene concept was first proposed by Crutzen and Stoermer (2000) and very soon became widely used. The term Anthropocene suggests that humankind is the main global geological force and the Earth has transitioned out of the Holocene epoch. Since the advent of the Anthropocene concept, it has become widely used in global change research groups and mass media (Steffen et al., 2011) and has brought with it the question of where its boundary should be placed (Zalasiewicz et al., 2015; Brown et al., 2017).

It is necessary to consider some indicators of environmental change and to figure out the stratigraphic signals that can be characterize the Anthropocene (Waters, 2014). The first proposal for the Anthropocene was based on the beginning of the increases in global carbon dioxide and methane trapped in polar ice, and it was suggested that the start of the Anthropocene could be set in the latter part of the eighteenth century, corresponding to the beginning of the Industrial Revolution (Crutzen, 2002). As is well known, stratigraphy provides insights into the dynamics and evolution of the Earth's system over the history of the planet (Steffen et al., 2016). Indicators in sediment that are influenced by humans, such as polycyclic aromatic hydrocarbons (PAHs), heavy metals (Leorri et al., 2014), black carbon (BC), radioactive elements (Waters et al., 2016), and plant macrofossils (Stankevica et al., 2015), among others, can all be used to define the Anthropocene. The Anthropocene can also be defined based on diverse paleontological criteria, such as the mixtures of native and non-native species (Barnosky, 2013), human-impacted speciation rates (Thomas, 2015) and the changes in entire ecological communities (Pennisi, 2015). However, the conclusions that are based on these various indicators regarding the start of the Anthropocene are not consistent (Table 1).

The various start dates need to be systematically assessed against the requirements of a "golden spike" that must correspond to a global

* Corresponding authors.
E-mail addresses: gaochuanyu@iga.ac.cn (C. Gao), wangguoping@iga.ac.cn (G. Wang).

http://dx.doi.org/10.1016/j.ecolind.2017.09.040
Received 2 June 2017; Received in revised form 18 September 2017; Accepted 23 September 2017

Table 1
The indicators used to date the Anthropocene over the World.

Location	Indicators	Date time	Reference
Global	CO_2, CH_4	1784 CE (Common Era)	Crutzen (2002)
Global, Eurasia, Northeastern Canada	CO_2, CH_4, agriculture, forest clearance	Thousands of years ago	Ruddiman (2003)
Global	CO_2	1800 CE, stage 1 of Anthropocene	Steffen et al. (2007)
Global	Subsurface structures and fossils	1863 CE	Williams et al. (2007)
Global	Artificial radionuclides	1945 CE	Zalasiewicz et al. (2010, 2015)
America	CH_4	13,400 years BP (Before Present)	Smith et al. (2010)
Global	Sediment flux	3000 years BP	Syvitski and Kettner (2011)
Global	Anthropogenic soil	last c.2000 years of the late Holocene	Certini and Scalenghe, 2011
Global	Palaeontology	1950 CE	Barnosky (2013)
All continents except Antarctica	Sedimentation erosion rate	At least 2300 years BP	Brown et al. (2013)
Global	Ignition of fire	> 1.8 million years ago, early Anthropocene	Glikson (2013)
Remote arctic and alpine lakes	N stable isotope, siliceous microfossil	1850 CE	Wolfe et al. (2013)
Northern Spain	Atmospheric pollution, PAHs, heavy metal	ca. 1800 CE	Leorri et al. (2014)
Yellow River Basin, China	Soil, charcoal, pollen and archaeological data	~11,500–7000 BP, early Anthropocene	Zhuang and Kidder (2014)
Europe	Plant speciation	Not to mention	Thomas (2015)
Global	CO_2, bomb spike	1610 or 1964 CE	Lewis and Maslin (2015)
Global	Species	6000 years ago	Pennisi (2015)
Latvia	LOI, heavy metal, plant macrofossil	Not to mention	Stankevica et al. (2015)
Argentina	Sediment rate	Past two centuries ago	Forte et al. (2016)
Global	Stratigraphic and Earth system	Mid-20th century	Steffen et al. (2016)
Global	Geochemical, carbon, climate	1950 CE	Waters et al. (2016)
Global	Stratigraphical signal	Mid-20th century	Williams et al. (2016)
Global	Geomorphology	Not to mention	Brown et al. (2017)

stratotype section and point (GSSP) (Lewis and Maslin, 2015), and the best global standard stratigraphic age (GSSA) to date the start of the Anthropocene should be determined via site sampling in regional perspective. The anthropogenic change throughout China, Korea, the Russian Far East, and Japan became increasing pervasive was mainly driven by global warming near the end of Pleistocene time (Aikens and Lee, 2013). Both the history of the Yellow River region (Zhuang and Kidder, 2014; Kidder and Zhuang, 2015; Rosen et al., 2015) and Yangtze River region (Yang et al., 2002; Shu et al., 2010; Dearing et al., 2012) of China were mainly shaped by the human modification of the environment. The anthropogenic changes of the Yellow River region start slowly based on the soil, charcoal, pollen and archaeological data in the Early Holocene (~11,500–7000 before present), which can be called "the Early Anthropocene" (Zhuang and Kidder, 2014). Unlike the time framework above, Dearing et al. (2012) focused on that the recent rapid economic growth and population increases of Yangtze River region, which were strongly coupled to environmental degradation. The lake ecosystem has significantly shifted since the 1950s based on diatom records (Dong et al., 2015) and paleolimnological data (Xu et al., 2017) in this region.

Wetland sediments are readily and economically accessible geological archives for the study of climate changes and human activities, and their autochthonous mode of accumulation renders them less susceptible to redeposition (Chambers and Charman, 2004). Regional human activities in the Sanjiang Plain, Northeast China started to influence the amount and characteristics of biomass burning residuals (i.e., BC fluxes and PAHs) about a thousand years ago based on Cong et al. (2016)'s study of wetland sediments. These patterns were followed by an even sharper increase in BC fluxes during the last 150 years (Gao et al., 2014c), in conjunction with the enrichment factors (EFs) of heavy metals (Gao et al., 2014b). However, increasing concentrations of heavy metals cannot cause obvious changes to the ecological balance of wetland systems because of the resilience of those ecosystems. "Resilience" is the capacity to recover from a disturbance even though the biomes and ecological processes have been diminished (Holling, 1973; Müller et al., 2015). It is therefore necessary to include some biological indicators to detect when human activities break the balance of a wetland ecosystem. The start of human-modified ecological characteristics in wetland ecosystems could be regarded as the start of the Anthropocene (Dong et al., 2015; Xu et al., 2017).

Here, we conduct a comprehensive analysis of sedimentological parameters (sedimentation rate and grain size), geochemical features (heavy metals, BC fluxes and PAHs) and a biological indicator (plant macrofossils) that accumulated about a two hundred year period on the Sanjiang Plain, Northeast China. Combining these data with the historical human activities that are recorded in historical documents, the transition from the Holocene to the Anthropocene can be identified. In all, the objectives of this study are to (1) reveal the sedimentological parameters and geochemical features influenced by human activities, (2) detect the breakpoint in the plant community, and (3) evaluate the timing of the beginning of the Anthropocene in this region.

2. Material and methods

2.1. Study area and sampling

The Sanjiang Plain is a low and flat alluvial plain crossed by the Heilong River, Songhua River and Wusuli River (Fig. 1). The Heilong River and Wusuli River are the boundary rivers between China and Russia, and the southern Wusuli River originates from Xingkai Lake and flows north to merges into the Heilong River near Boli city. The Songhua River is one of the major rivers in China, and it originates in the Changbai Mountain and merges with the Heilong River near Tongjiang County. On account of the unique topography and climate, a large number of wetlands have developed in this area. During the last 150 years, there were three phases of exploitations of the Sanjiang Plain (Fig. 7d) (Fang et al., 2005). During the first phase, some areas of wasteland were turned into farmland with the gradual lifting from 1840 onward of executive limits previously imposed by the Qing dynasty. The second exploitation began in 1898 as a result of Russia's construction of the "Mid-east" Railway, during which a large number of forests were cut down and some minerals were exploited. Even after the second phase, at the beginning of New China phase, the Sanjiang Plain remained famous as "the great northern wildness" due to the large number of wetlands in this area. However, owing to the rapid increases in population and land exploitation that were encouraged and financed by the government, the wetland areas have decreased by more than 3/4 between 1954 and the present during the third phase of exploitation (Wang et al., 2009).

Four well-preserved wetlands surrounding the rivers and one wetland nearby the city were found on the Sanjiang Plain (Fig. 1). The Heixiazi (HXZ, 134°44′45″ E, 48°19′51″ N) wetland is located in a delta

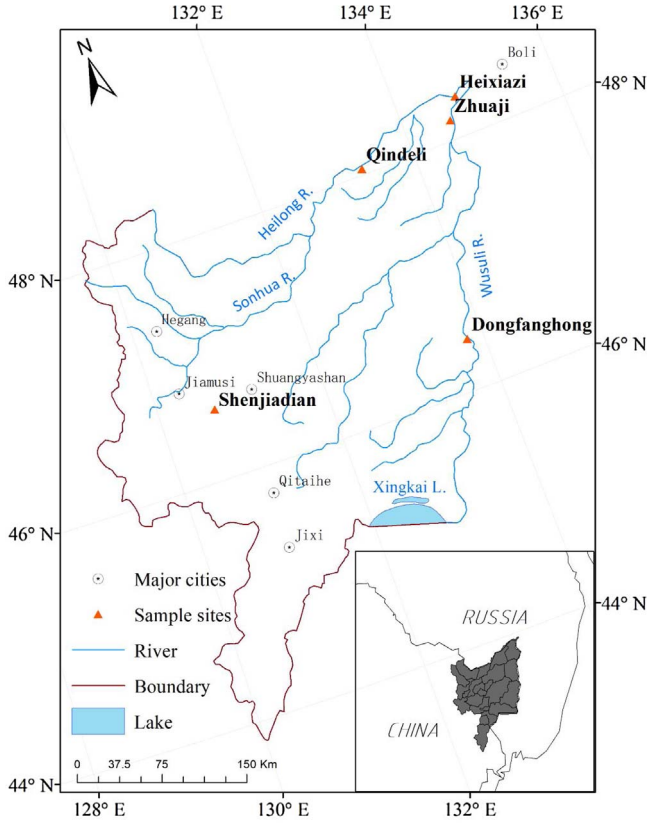

Fig. 1. Study area and location of the sampling sites.

region where the Heilong and Wusuli rivers converge, the Qindeli (QDL, 133°20′31″ E, 48°2′1″ N) wetland is close to the HXZ wetland but is located upstream along the Heilong River. The Dongfanghong (DFH, 133°37′34″ E, 46°23′44″ N) and Zhuaji (ZJ, 134°37′43″ E, 48°9′36″ N) wetlands are located along the Wusuli River. The Shenjiadian (SJD, 130°39′52″ E, 46°34′52″ N) wetland is a typical valley peatland (comprising 57.5% mean organic matter, Supplementary data) in Huachuan County, approximately 34 km from the major city of Jiamusi. Detailed site descriptions of the QDL and SJD wetlands were provided in Gao et al. (2014a), and the HXZ, ZJ and DFH wetlands were described in Gao et al. (2014b). In the central region of each wetland, cores were collected using a Russian peat corer. The profiles were cut into contiguous 1-cm samples in the field using a stainless steel knife, and the samples were sealed in tagged plastic bags for transport to the laboratory and refrigerated at −20 °C for further analysis

2.2. Multi-proxy analyses

2.2.1. Chronology and sedimentation rates

Sub-samples were dried in an oven at a temperature of 105 °C for 12 h and were ground through a 100-mm mesh. The radioactive strength of ^{210}Pb was measured at the State Key Laboratory of Lake Science and Environment, Nanjing Institute of Geography and Limnology of the Chinese Academy of Sciences (CAS). The age framework was established using the constant rate of supply model (CRS) (Goldberg and Koide, 1963; Appleby and Oldfield, 1978).

The sedimentation rate was calculated based on the thickness of the sediment accumulation over a unit of time. An increasing sedimentation rate due to soil erosion in farmlands or other sites reflects human-induced accumulation processes (Forte et al., 2016). It is important to quantify the sedimentation rate to understand the changes that are driven by natural and human-induced factors (Cahoon and Turner, 1989). The sedimentation rate for each profile was calculated for the peat layers between the dated depths of the profiles. The following equation was used: $r = h/t$, where r is the sedimentation rate (cm/yr); h is the thickness of sediment (cm); t is the accumulation time (yr). The method of determine sedimentation rate is based on the sediment depth-age framework (Robbins and Edgington, 1975; Goudie and Viles, 2016). This simple approach meets our demand for analysis the human impact on the sediments.

2.2.2. Grain size analysis

The grain size of sediment has been used as an indicator of the intensity of soil erosion, with coarser grains typically interpreted as representing a higher intensity soil erosion that corresponds to human activities near the site (Goudie and Viles, 2016). Sub-samples were burnt at 550 °C in a muffle furnace for 4 h to eliminate organic matter, and a Malvern Mastersizer 2000 laser grain-size analyzer was used at the Analysis and Test Center of the Northeast Institute of Geography and Agroecology (IGA), CAS. The measurements were automatically performed 3 times (6 s each time) for each sample to obtain an average value (Tian et al., 2013).

2.2.3. Heavy metal, BC and PAHs analyses

Heavy metals (e.g., Cu, Zn and Pb) are easily increased by regional human activities (e.g., mining, fossil fuel burning, industrial discharge and pesticide use), and the EF is a useful tool for evaluating historical anthropogenic pollution (Gallego et al., 2013). Atomic emission spectrometry with inductively coupled plasma (ICPS-7500, Shimadzu, Japan) was used to determine the metal content at the Analysis and Test Center of IGA, CAS. Standard reference materials (GBW07401) were obtained from the Chinese Academy of Measurement Sciences, and the recovery rates for elements were approximately 93–109%. For the calculation of the EFs of the heavy metals (e.g., Cu, Zn and Pb), V, Ti and Zr were used as conservative elements (Gao et al., 2014b). BC is produced by the incomplete combustion of fossil fuels or biomass and can be stored in the soil for thousand years (Hammes et al., 2007). The study of BC in sediments can therefore be used to understand the anthropogenic or natural emission intensity. BC in the wetland sediments was measured via the dichromate oxidation method developed by Song et al. (2002), and details of the analysis can be found in Gao et al. (2014c) and Cong et al. (2016). PAHs are organic pollutants in the sediments, and many of them come from the human-related combustion of fossil fuels (Khairy et al., 2009). Hence, the PAHs are also suitable for identifying the history of human activities. The extraction procedure for PAHs is referenced from Khim et al. (1999), and the PAHs were quantified using a gas chromatogram and mass spectrometer system (GCMS-QP5050A, Shimadzu, Japan) following the description in Cong et al. (2016).

2.2.4. Plant macrofossils analysis

Plant macrofossils were analyzed using the quadrat and leaf count protocol (Barber et al., 1994) to determine the plant community succession in the sediments. Sub-samples of 5 cm^3 were taken at 2-cm intervals in the SJD peatland, which has abundant organic matter and various plant species. At this site, we were able to identify more plant macrofossils than in other cores to better study the plant community succession. The methods for preparing the sub-samples and the details of the species identification can be found in Wang et al. (2015), in which the focus was on the water level changes that was reflected by plant macrofossils over long time scales. The plant macrofossil diagram was created using R software (v 3.0.3) with the rioja library package, and the zones were determined by cluster analysis (Juggins, 2017).

2.3. Statistical methods

2.3.1. Principal component analysis

Principal component analysis (PCA) can be used to reduce the dimensionality of a data set in which there are a large number of

interrelated variables (Jolliffe, 1986). The first principal component scores (PC1-scores) represent the most important information from the data set and can be used to analyze the shifts in the variables. Linear interpolation was applied to the sedimentological parameters, geochemical features and plant community of the wetlands to obtain variables of equal age. After that, the variables were transformed to Z scores by the following equation: Z-score = $(X_i\text{-}X_{avg})/X_{std}$, where X_i is the given value of a raw variable, and X_{avg} and X_{std} are the average and standard deviation of the variables, respectively. The Z-scores were analyzed by using PCA in CANOCO (version 4.5) to extract the principal component, and the PC1-scores were plotted against the age. We also drew a biplot of the PC1 and PC2 scores of plant macrofossils from the SJD profiles, and the PC1scores generally reflected the main aspects of the changes in the plant community.

2.3.2. Ecosystem breakpoint detection

The plant community is the basis of an ecosystem and an important measurement index for the development level of a wetland. To identify structural changes in a plant community, the F statistics-age graph was plotted in R software using the “strucchange” package in linear regression models from F test framework (Zeileis et al., 2002), and the breakpoint of an ecosystem was estimated by the fluctuation in the F statistics.

3. Results

3.1. Age-depth model and sedimentological parameters

The radioisotope results for ^{210}Pb in the sediments of the wetlands are plotted against depth in Fig. 2. The activities of ^{210}Pb generally showed exponentially decreasing trends with depth and reached relatively stable values at the deepest depth of the cores. The SJD, DFH, ZJ, HXZ and QDL records obtained from the cores represent time spans of 180 yr, 97 yr, 144 yr, 122 yr and 162 yr, respectively, using of the CRS model (Fig. 3). Detailed information on the sedimentation rates and mean grain sizes with depth was plotted together in Fig. 3. The annual average sedimentation rate was the highest in the QDL wetland (0.49 ± 0.30 cm/yr), and the lowest in the DFH wetland (0.18 ± 0.08 cm/yr). There were no differences in the ZJ and HXZ wetlands (0.31 ± 0.15 cm/yr), or in the SJD wetland (0.41 ± 0.29 cm/yr). The annual average median fraction sizes showed pronounced variation ranging between 10 ± 1.13 μm (DFH) and 49.71 ± 17.49 μm (SJD) (Table 2).

3.2. Geochemical features

The change characteristics of heavy metal EFs, BC fluxes and PAHs concentrations with age are shown in Fig. 4. The mean EFs of Cu (1.90 ± 0.30), Zn (1.83 ± 0. 51) and Pb (1.49 ± 0.19) in the DFH wetland were the highest, and the lowest mean EFs of Cu (1.32 ± 0.16), Zn (0.88 ± 0.46) and Pb (0.84 ± 0.33) were in the HXZ, QDL and SJD wetlands, respectively. Compared to the DFH (0.44 ± 0.21 mg/yr/cm^3) and HXZ (0.65 ± 0.45 mg/yr/cm^3) profiles, the mean BC flux in the SJD peat profile (2.90 ± 2.52 mg/yr/cm^3) was the highest with a large variation between the maximum (12.26 mg/yr/cm^3) and minimum (0.16 mg/yr/cm^3). The mean PAHs concentrations in the SJD (0.48 ± 0.20 μg/g) and DFH (0.41 ± 0.48 μg/g) wetlands were approximately the same, and the mean value was higher in the HXZ core (0.62 ± 0.32 μg/g) than in the other cores (Table 1).

3.3. Plant macrofossils

Fig. 5 shows the percentages of plant macrofossil found in the SJD peatland sedimentary successions over the past 200 years (0–40 cm depth). These data allowed for a detailed reconstruction of the local plants, and the macrofossil results in this study are different from our previous work (Wang et al., 2015). We focus on hundreds of years of plant community changes, while the previous research emphasized changes on the scale of thousands of years. Therefore, the age framework, as well as the macrofossil content description, is different between the two studies despite the use of the same core. Three main zones were identified based on a cluster analysis of the plant macrofossil assemblages.

Zone A (1810–1950 CE) was dominated by *Carex lasiocarpa*, with low abundances of *Carex pseudocuraica*, *Menyanthes trifoliate* and *Carex* sp., which were not always present in the sediments. *Equisetum fluviatile* was almost absent throughout the zone, and *Carex pseudocuraica*, shrubs (mainly *Salix myrtilloides*, *Salix brachypoda* and *Betula fruticosa*) and brown moss appeared at several specific depths in this zone. There were stable low values of charcoal during this interval. This zone shows that species were in a relatively steady state, except for a sudden increase in *Chenopodiaceae* seeds in 1920 CE.

Zone B (1950–1980 CE). A steep decline in *Carex lasiocarpa* occurred from the 1950s in this zone. Charcoal showed a minor increase. *Carex pseudocuraica* was found at the beginning of this zone and subsequently almost disappeared. There was a decrease in *Carex* sp., and

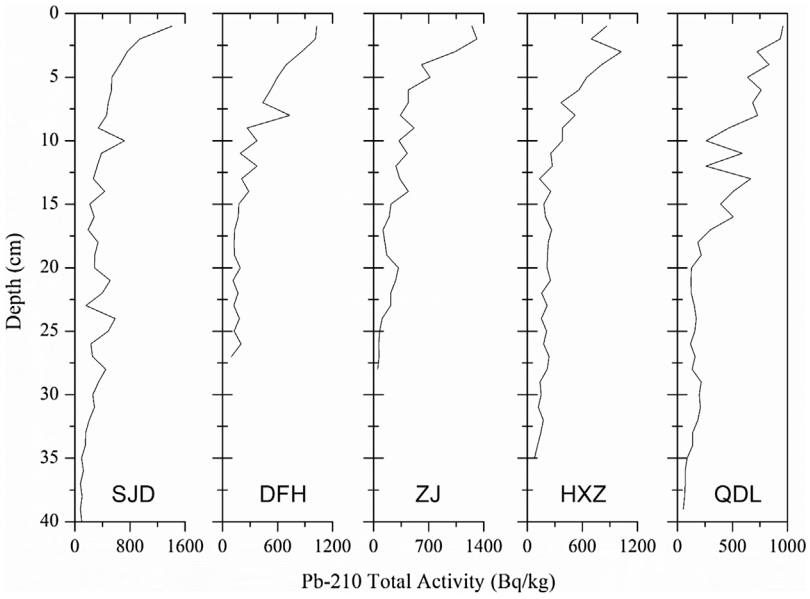

Fig. 2. ^{210}Pb activities plotted against depth in the five cores from the Sanjiang Plain, Northeast China.

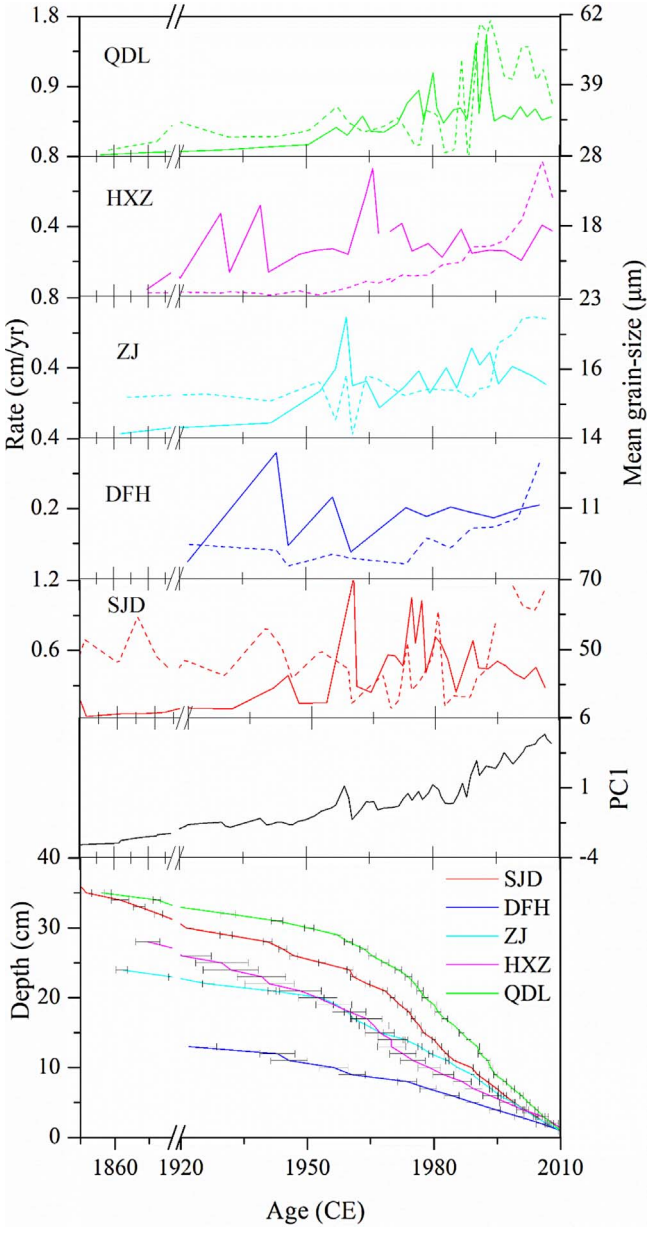

Fig. 3. Age-depth frame derived from ^{210}Pb activities by the CRS model and the variations of sedimentological parameters. The sedimentation rate (solid line) and mean grain size (dash line) of the profiles, accompanied by the first principal component scores.

the amount of *Carex* sp. was variable compared to the previous period. *Menyanthes trifoliate* experienced a slight increase, and small amounts of *Chenopodiaceae* and *Cyperaceae* seeds fluctuated throughout this zone.

Zone C (1980–2010 CE). There was a significant decline in *Carex lasiocarpa* in this zone to a point where it was almost absent. Shrub remains (mostly *Salix myrtilloides*) and charcoal rapidly increased, and reached a maximum at the top of the profile. *Menyanthes trifoliate*, *Carex* sp., moss and *Cyperaceae* seeds almost disappeared in this period.

4. Discussion

4.1. The sedimentary background under the influence of humans

The sedimentation rates were stable before 1950 in the cases of the SJD and ZJ wetlands, and higher values appeared after this period in these two wetlands (Fig. 3), which may have been caused by the third exploitation period after the founding of New China in the 1950s. In the third exploitation period, a large number of farmers, demobilized military and educated youth moved to this area in succession, and the population increased from 1.40–8.52 million between 1950 and 2000 CE (Liu and Ma, 2002); the land reclamation rate also increased to 33.5% during this time (Research group on Chinese wetland development and protection, 1998). The state macroscopic agricultural policies played an important role in the increase in the farmland area (Song et al., 2008). The land reclamation in this period caused so much soil erosion that more soil dust was captured by the wetlands, leading to an obvious increase in wetland sedimentation rates. The mean grain size exhibited an increasing trend in the 1980s in the SJD, DFH and QDL wetlands, and a similar increasing trend was seen in the ZJ wetland in the 1990s (Fig. 3). Marked development and construction has occurred in both agriculture and industry since the Chinese economic reform in 1978 CE The major method of agricultural production on the Sanjiang Plain has gradually changed and agricultural mechanization has become widely used for planting and reaping. Consequently, soil erosion caused by agricultural mechanization was more serious in this period. Unlike the mean grain sizes in other wetlands, the gradual increase in mean grain size values started in 1950 CE (Fig. 3) in the HXZ wetland, which is located at the convergence of the Heilong and Wusuli rivers, and the sedimentary processes were influenced by these two rivers.

The PC1 scores (λ = 0.45) of the sedimentation rates and mean grain sizes from the five wetlands can be regarded as the sedimentary index for the Sanjiang Plain over the last 150 years. The PC1 scores had an obvious increasing trend throughout the whole phase. Increasing PC1 scores mean that the sedimentation rates and mean grain sizes on the Sanjiang Plain increased over the last 150 years and also indicate more and more strongly that these increases were influenced by regional human activities; thus, a higher value of sedimentary index means a higher degree of human activities in this region. There was a higher value for the sedimentary index in approximately 1954 CE, which was followed by a gradually increasing trend until 1980 CE (Fig. 3) and reflects the third exploitation in the Sanjiang Plain. After that, the more rapidly increasing trend of the sedimentary index indicates that the intensity of the human activities increased with further development after the reform and opening up in China.

4.2. Historical pollution and combustion dominated by humans

The SJD peatland is close to the Jiamusi City (Fig. 1) and can be

Table 2
Comparison of mean values and standard deviation of recent sediment rate, mean grain-size, black carbon, polycyclic aromatic hydrocarbons and the enrich factors of heavy metal at the five investigated sites in the Sanjiang Plain, Northeast China.

Sample sites	Age (yr)	Sediment rate (cm/yr)		Grain-size (μm)		BC (mg/yr/cm^3)		PAHs (μg/g)		Cu_{EFs}		Zn_{EFs}		Pb_{EFs}	
		Mean	Std	Mean	Std	Mean	Std	Mean	Std	Mean	Std	Mean	Std	Mean	Std
SJD (n = 36)	180	0.41	0.29	49.71	17.49	2.90	2.52	0.48	0.20	1.58	0.49	1.35	0.63	0.84	0.33
DFH (n = 14)	97	0.18	0.08	10	1.13	0.44	0.21	0.41	0.32	1.90	0.30	1.83	0.51	1.49	0.19
ZJ (n = 24)	144	0.31	0.15	15.02	3.08	/	/	/	/	1.37	0.32	1.28	0.24	1.36	0.24
HXZ (n = 27)	122	0.31	0.15	11.71	4.60	0.65	0.45	0.62	0.48	1.32	0.16	1.36	0.30	1.30	0.18
QDL (n = 34)	162	0.49	0.30	32.28	13.46	/	/	/	/	1.87	0.77	0.88	0.46	1.04	0.50

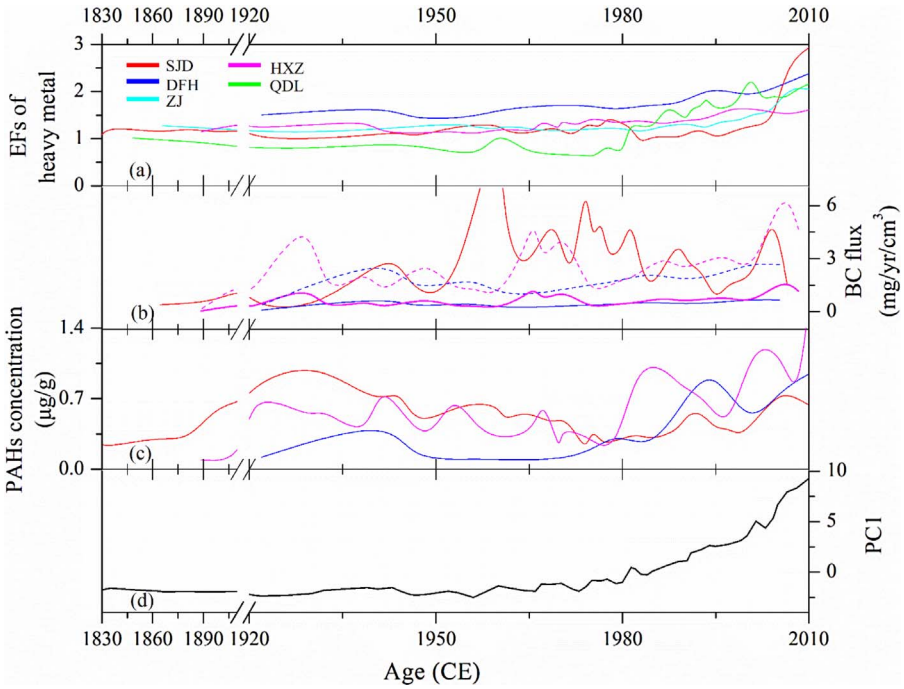

Fig. 4. Geochemical features of the sediments. (a) The enrich factors of heavy metals (average value of Cu, Zn and Pb) in the five wetlands; (b) black carbon fluxes in the SJD (Gao et al., 2014c), DFH and HXZ wetlands (Cong et al., 2016), and the values of DFH and HXZ were quadrupled and plotted in the graph (dash line); (c) the concentrations of polycyclic aromatic hydrocarbons in the SJD, DFH and HXZ wetlands (Cong et al., 2016); (d) first principal component scores of the geochemical features.

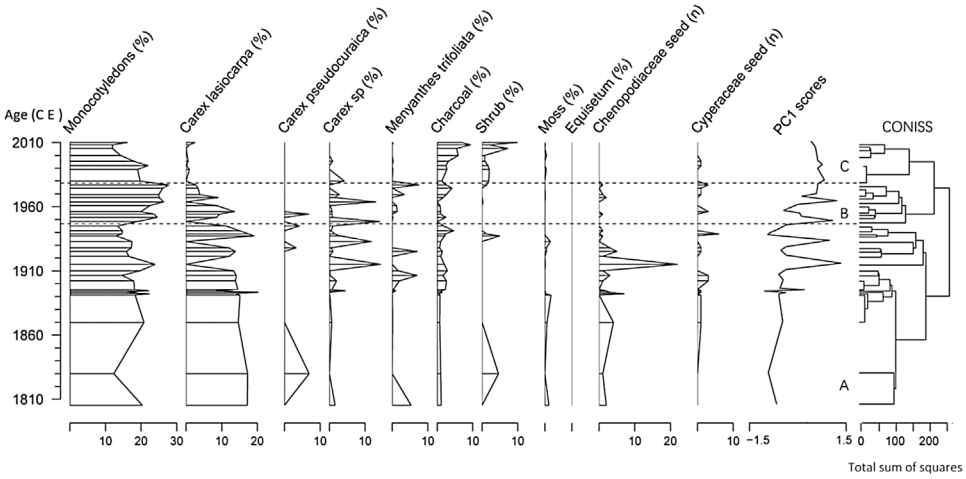

Fig. 5. Plant macrofossils diagram (percentages, numbers) of SJD peat core shown together with ages. Total sum of squares is the result of cluster analysis and three main zones (A/B/C) were identified in our data.

easily influenced by human activities. There was a slowly increasing trend in the EFs of heavy metals from the 1980s to the 2000s and a dramatic increase after 2000 CE (Fig. 4a). The heavy metals might have come mainly from pesticide contamination, and the pesticide production reached 53.7 × 10^4 t, the highest on record in China in 1980 CE (Hua and Shan, 1996), which coincided with a marked development in agriculture after China's reform and opening up. Biomass burning and industrial pollution, as evidenced by the concentrations of PAHs in the SJD wetland, increased from 1840 CE and reached a maximum in approximately 1935 CE (Fig. 4c) which might have been caused by the first and second exploitations of the Sanjiang Plain and some mining that started in these periods. The BC fluxes sharply increased from 1950 CE and reached a maximum in 1960 CE then dynamically declined until 1995 CE, during the third exploitation. The proximal location of the SJD wetland to a city meant that it was influenced by more industrial pollution than the wetlands that are farther away from city areas. Although the BC fluxes in the SJD wetland showed a dynamic declining pattern, the values were still higher than those in the DFH and HXZ wetlands (Fig. 4b).

Two of the five wetlands, QDL and HXZ, are located along the Heilong River. Samples taken in the QDL wetland in the upstream region of the Heilong River showed higher values for EFs of heavy metals than those taken in HXZ after 1980 CE This pattern could indicate that human activities started to lead to the deposition of more heavy metals into the QDL wetland starting in 1980 CE However, the EFs of heavy metals in the HXZ wetland in the downstream region of the Heilong River almost showed stable patterns in all stages, with only a gradual increasing from 1965 CE (Fig. 4a). This pattern might be due to the fact that heavy metal concentrations can decrease gradually with the water flow because of the self-purification of the water body and sedimentation processes (Ostroumov, 2002; Vagnetti et al., 2003).

There were fairly similar increasing trends of EFs from 1954 CE in the DFH and ZJ wetlands, which are both situated along the Wusuli River. The BC fluxes and the concentrations of PAHs had higher values in approximately 1945 CE then showed an increasing trend from 1960 CE in the DFH wetland (Fig. 4b, c). This similar trend indicates that human activities have intensively affected this area's wetland environments from the 1950s, which agrees with the fact that Jixi City began to develop many coal mines from the 1950s onward (Luo et al., 2007) that caused serious wastewater pollution and decreased the water quality in the Wusuli River area (Gao et al., 2014b). Historical trends of PAHs concentrations in the DFH and HXZ wetlands were fairly

similar to those in the city-proximal SJD wetland before 1980 CE, and then showed a dynamical increase after the 1980s (Fig. 4c). Atmospheric PAHs exist mainly in the gaseous form, which favors long-range transport from the source (Berset et al., 2001). Similar variations in the PAHs concentrations in these three wetlands confirmed the historical influence changes of human activities.

Human activities in the city-proximal wetland (SJD) and Wusuli River area (DFH and ZJ) started to strengthen in the 1950s, and the human activities in the Heilong River area (QDL) were relatively weak until 1980 CE Based on the regional economic development history, the exploited areas were mainly distributed in the south and west of the Sanjiang Plain, and the north Heilong River area was developed later (Fang et al., 2005). The higher values of heavy metals, BC fluxes and PAHs indicate high-intensity human activities, so the higher PC1 scores (geochemical index of the Sanjiang Plain, $\lambda = 0.45$) represent a strengthening of human activities. The geochemical index was stable before 1954 CE and slowly increased until 1980 CE, after which the geochemical index showed a sharply increasing trend (Fig. 4d). Overall, the geochemical index increased after 1954, meaning that the intensity of regional human activities increased significantly after the third exploitation.

4.3. Plant community succession with the human impact

The SJD peatland is located in a valley near Shenjiadian Village on the Sanjiang Plain, and the plant community is primarily controlled by the semi-humid continental monsoonal climate in the warm temperate zone. The plant community succession can be influenced by various natural and artificial factors, especially low water levels due to anthropogenic drainage for farmland reclamation (Marques et al., 2004) or high nutrient inputs caused by industrial and residential sewage pollution (White and Bayley, 2001).

During the 200 years of the plant community history, the SJD peatland was initially a typical *Carex lasiocarpa* peatland. Around the 1950s, the percentage of *Carex lasiocarpa* showed a sudden decrease, and charcoal and shrubs showed increasing trends (Fig. 5). High proportions of shrubs and decreasing proportions of *Carex lasiocarpa* indicated that the water level decreased in approximately the 1950s (Lou et al., 2013). However, the rainfall data collected from weather stations across the Sanjiang Plain suggest that this place was wetter in the 1950s than in other periods (Luan et al., 2007). Therefore, the main reason that the water level in the SJD peatland decreased was due to drainage of the peatland for exploitation or more underground water use for agriculture (Wang et al., 2009), rather than a drying climate or limited rainfall. The increase in charred macrofossils, BC and PAHs suggested that frequent local fires occurred, which is in agreement with the result found by Zhang et al. (2015). This phenomenon could be related to local farm reclamation that involved setting fire to the grass; and suggests that human activities caused more fire events and became more intensive in this area since the 1950s.

The PC1 scores (plant index, $\lambda = 0.47$) represented the major variation trend in the plant community, and a shift in the plant index reflects a fluctuation in the wetland ecosystem. The SJD peatland system showed a sudden change in 1948 CE and reached the breakpoint in approximately 1960 CE (Fig. 6b) based on the F statistics of the structural changes test. There were remarkable differences among the plant communities in 1948 CE (Fig. 6a) based on the PCA ordination of the samples. The sudden change in the ecosystem occurred in the third exploitation due to the stronger influence of human activities.

4.4. The timing of the beginning of the Anthropocene on the Sanjiang plain

According to our stratigraphic results and the historical records, the anthropogenic activity on the Sanjiang Plain can be divided into five periods within the three exploitations: the original period, the initial ban-lifting period, the *trans*-Siberian Railroad period, the Japanese occupation period, and the New China period (Fig. 7d). The sedimentary index, geochemical index and plant index data presented in the previous discussion section were selected evaluate the influence of regional human activities during these five periods on the wetland ecosystem on the Sanjiang Plain (Fig. 7b–d).

The Sanjiang Plain was protected by the government during the Qing Dynasty, and the limited number of immigrants to this region led to a much lower degree of development in agriculture and industry compared to other areas in southern China (Xue and Li, 1993). The sedimentary index, geochemical index and plant index were all negative during this period (Fig. 7b–d). With the lifting of the entry ban, the increase in immigrants led to the development of agriculture and an increase in produce farming, providing the foundation for the development of business (Li, 2005). Although population growth promoted the development of land reclamation on the Sanjiang Plain, the percentage of land reclamation was only 2.07%, due to the vast nature of the territory with its sparse population and short development history before 1912 CE (Research group on Chinese wetland development and protection, 1998). The stratigraphic results showed that the three different indexes were low and stable in the original time and the initial ban-lifting period before 1898 CE (Fig. 7b–d), suggesting that the degree of anthropogenic influence on the wetland sediments was at near background levels in these two periods.

Massive forests were chopped down along the Heilong and Wusuli rivers, and more minerals were exploited for the construction of the Mid- East Railway starting in 1897 CE Businesses developed rapidly after the railway was completed in 1903 CE, and some cities and towns developed along the railway (Fang et al., 2005). Moreover, the forests and minerals (e.g., coal resources) were rapidly exploited when the Sanjiang Plain was occupied by the Japanese since 1932 CE (Liu, 1987). For this reason, the sedimentary index rose even more rapidly, and the forest declined sharply during this period. The plant index had some sudden shifts in approximately 1905 CE, 1931 CE and 1945 CE that might coincide with the timing of several wars (the Russo-Japanese war, the Japanese invasion of Northeast China and the USSR war against Japan) (Fig. 7d). The gradually increasing trends of the sedimentary and plant indexes (Fig. 7b, d) indicate that the wetland system changed slightly between 1897 CE and 1945 CE, which agrees with the second exploitation.

After the establishment of New China, the economy needed to develop on the Sanjiang Plain. People were encouraged to migrate to this region, and the population increased faster than before 1950 CE onward (Fig. 7a). The increasing trends of the sedimentary and geochemical indexes were steeper from approximately 1950 CE onward than previously. The plant index also reached a peak, and the plant community transitioned from *Carex lasiocarpa* to *Salix myrtilloides* in 1950 CE Based on sedimentary, geochemical and plant indexes, the intensive influence of anthropogenic activities on wetland sediments mainly started in the 1950s, and we suggest that the 1950s can be treated as the start time of the Anthropocene on the Sanjiang Plain, Northeast China.

We are not the first to suggest that the Anthropocene began in the 1950s, as this start date was settled on by most global researchers from the Working Group on the Anthropocene at the 35th International Geology Conference, which was held in Cape Town, South Africa in 2016. However, it remains controversial. To formalize the Anthropocene as a geological epoch is a complex question, and determining the stratigraphic signals plays an important part in the processes of defining the Anthropocene. Paleoenvironmental proxy records of lakes in the Yangtze River Basin, East China indicated the agricultural activities were intensified since the 1950s and the lake ecosystems were degraded (Dearing et al., 2012; Dong et al., 2015), which showed significant synchronous changes in the intensity of the human activities on the Sanjiang Plain, Northeast China.

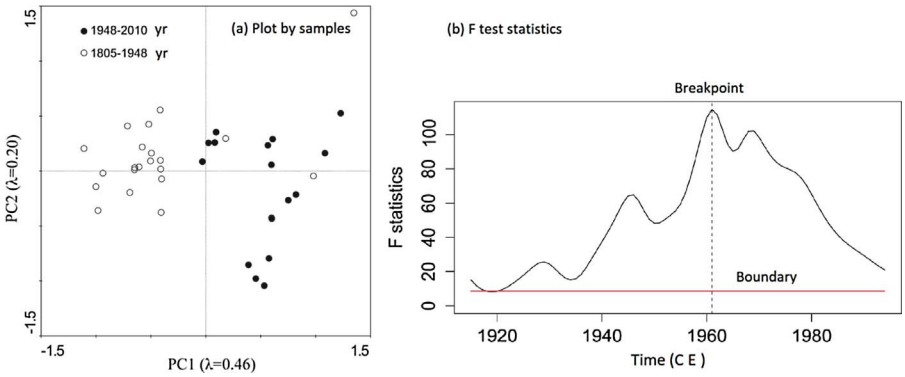

Fig. 6. The structure change of the plant community in the SJD peatland. (a) Biplot of the PC1 and PC2 scores ordination of plant macrofossils from SJD profiles; (b) Breakpoint of plant community detected by F test statistics. The red line means the boundary of the F statistic values, and the fluctuation of F statistics is the largest around 1960C.E. (For interpretation of the references to colour in this figure legend, the reader is referred to the web version of this article.)

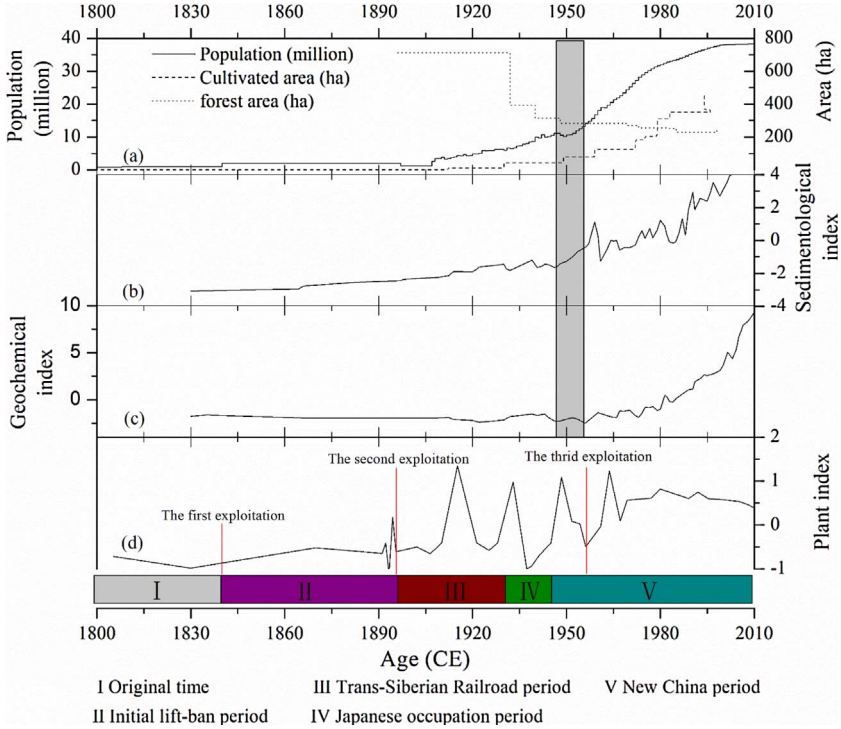

Fig. 7. The comparison of stratigraphic indicators and historical records. (a) historical population of Heilongjiang Province (solid line), cultivated area changes of the Sanjiang Plain (dash line) and forest area changes of the Sanjiang Plain (dot line); (b–d) the first principal component scores of sedimentological parameters, geochemical features and plant indicator, respectively, and the periods of anthropogenic activities recorded by documents in the Sanjiang Plain, and the red straight line represent the beginning time of the exploitation. (For interpretation of the references to colour in this figure legend, the reader is referred to the web version of this article.)

5. Conclusions

The sedimentary background seems to reflect the anthropogenic geomorphic changes on the Sanjiang Plain, Northeast China. The sedimentation rates in most cores were much lower and the mean grain sizes were much finer at the original time point and during the initial ban-lifting period. Historical pollution and combustion predominately caused by people resulted in small changes during the building of the *trans*-Siberian Railroad and the Japanese period of occupation. Since the founding of New China (1949 CE), the sedimentary background parameters and geochemical features all showed abrupt changes.

There was a succession of plant communities in the SJD peatland, which transitioned from a *Carex lasiocarpa* community to a *Salix myrtilloides* community after the 1950s. The PCA scores ordination and the ecosystem breakpoint based on plant macrofossils showed that the ecosystem experienced a change between 1948 and 1960 CE

The start of the Anthropocene on the Sanjiang Plain, Northeast China, was evaluated by stratigraphic indicators, such as sedimentological parameters (e.g., sedimentation rate and grain size), geochemical features (e.g., heavy metals, BC and PAHs) and a biological indicator (plant macrofossils). Based on these data, and in combination with the history of human activities, the regional ecosystem changes caused by human activities started in the New China period; thus, the start of the Anthropocene in this region can be set as the 1950s.

The concept of the Anthropocene remains open for debate. It is hard for the public at large or political leaders to perceive. However, the significant influence on the Earth's systems afforded by human activity is clear to all of us. We need to strengthen the research on the drivers of the Anthropocene to protect the viability of contemporary civilization into the future.

Acknowledgements

The authors gratefully acknowledge the assistance of the Analysis and Test Center, Northeast Institute of Geography and Agroecology, Chinese Academy of Sciences. This work was supported by the National Natural Science Foundation of China (No. 41571191, 41701217); and the national key research and development project (No.2016YFA0602301).

Appendix A. Supplementary data

Supplementary data associated with this article can be found, in the online version, at http://dx.doi.org/10.1016/j.ecolind.2017.09.040.

References

Aikens, C.M., Lee, G.A., 2013. Postglacial inception and growth of anthropogenic landscapes in China, Korea, Japan, and the Russian Far East. Anthropocene 4, 46–56.

Appleby, P.G., Oldfield, F., 1978. The calculation of Pb dates assuming a constant rate of supply of unsupported Pb to the sediment. Catena 5, 1–8.

Barber, K., Chambers, F., Maddy, D., Stoneman, R., Brew, J., 1994. A sensitive high-resolution record of late Holocene climatic change from a raised bog in northern England. Holocene 4, 198–205.

Barnosky, A.D., 2013. Palaeontological evidence for defining the Anthropocene. Geol. Soc. Lond. Spec. Publ. 395, 149–165.

Berset, J.D., Kuehne, P., Shotyk, W., 2001. Concentrations and distribution of some polychlorinated biphenyls (PCBs) and polycyclic aromatic hydrocarbons (PAHs) in an ombrotrophic peat bog profile of Switzerland. Sci. Total Environ. 267, 67–85.

Brown, A., Toms, P., Carey, C., Rhodes, E., 2013. Geomorphology of the Anthropocene: time-transgressive discontinuities of human-induced alluviation. Anthropocene 1, 3–13.

Brown, A.G., Tooth, S., Bullard, J.E., Thomas, D.S.G., Chiverrell, R.C., Plater, A.J., Murton, J., Thorndycraft, V.R., Tarolli, P., Rose, J., 2017. The geomorphology of the Anthropocene: emergence, status and implications. Earth Surf. Process. Landf. 42, 71–90.

Cahoon, D.R., Turner, R.E., 1989. Accretion and canal impacts in a rapidly subsiding wetland II: Feldspar marker horizon technique. Estuaries 12, 260–268.

Certini, G., Scalenghe, R., 2011. Anthropogenic soils are the golden spikes for the Anthropocene. Holocene 21, 1269–1274.

Chambers, F.M., Charman, D.J., 2004. Holocene environmental change: contributions from the peatland archive. Holocene 14, 1–6.

Cong, J., Gao, C., Yan, Z., Zhang, S., He, J., Wang, G., 2016. Dating the period when intensive anthropogenic activity began to influence the Sanjiang Plain, Northeast China. Sci. Rep. 6, 1–9.

Crutzen, P., Stoermer, E., 2000. The anthropocene. Glob. Change Newslett. 41, 17–18.

Crutzen, P.J., 2002. Geology of mankind. Nature 415, 23.

Dearing, J.A., Yang, X., Dong, X., Zhang, E., Chen, X., Langdon, P.G., Zhang, K., Zhang, W., Dawson, T.P., 2012. Extending the timescale and range of ecosystem services through paleoenvironmental analyses, exemplified in the lower Yangtze basin. Proc. Natl. Acad. Sci. U. S. A. 109, E1111–E1120.

Dong, X., Yang, X., Chen, X., Liu, Q., Yao, M., Wang, R., Xu, M., 2015. Using sedimentary diatoms to identify reference conditions and historical variability in shallow lake ecosystems in the Yangtze floodplain. Mar. Freshwater Res. 67, 803–815.

Fang, X.Q., Ye, Y., Ge, Q.S., 2005. History of land exploitation in the Northeast China during the Qing Dynasty inferred from the development of town system. Sci. Geogr. Sin. 25, 129–134 (In Chinese).

Forte, L.M., Hurtado, M.H., Dangvas, N.V., Couyoupetrou, L., Gimenez, J.E., da Silva, M.M., Bruschi, V.M., Cendrero, A., 2016. Anthropogenic geomorphic change as a potential generator of renewable geologic resources in the humid Pampa of Argentina. Catena 142, 177–189.

Gallego, J.L., Ortiz, J.E., Sierra, C., Torres, T., Llamas, J.F., 2013. Multivariate study of trace element distribution in the geological record of Ronanzas Peat Bog (Asturias, N. Spain). Paleoenvironmental evolution and human activities over the last 8000 calyr BP. Sci. Total Environ. 454–455, 16–29.

Gao, C., Bao, K., Lin, Q., Zhao, H., Zhang, Z., Xing, W., Lu, X., Wang, G., 2014a. Characterizing trace and major elemental distribution in late Holocene in Sanjiang Plain, Northeast China: paleoenvironmental implications. Quat. Int. 349, 376–383.

Gao, C., Lin, Q., Bao, K., Zhao, H., Zhang, Z., Xing, W., Lu, X., Wang, G., 2014b. Historical variation and recent ecological risk of heavy metals in wetland sediments along Wusuli River, Northeast China. Environ. Earth Sci. 72, 4345–4355.

Gao, C., Lin, Q., Zhang, S., He, J., Lu, X., Wang, G., 2014c. Historical trends of atmospheric black carbon on Sanjiang Plain as reconstructed from a 150-year peat record. Sci. Rep. 4, 1–7.

Glikson, A., 2013. Fire and human evolution: the deep-time blueprints of the Anthropocene. Anthropocene 3, 89–92.

Goldberg, E., Koide, M., 1963. Rates of Sediment Accumulation in the Indian Ocean. North-Holland publishing Company, Amsterdam.

Goudie, A.S., Viles, H.A., 2016. Hillslope processes in the Anthropocene. In: Goudie, A.S., Viles, H.A. (Eds.), Geomorphology in the Anthropocene. Cambridge University Press, Cambridge, pp. 71–86.

Hammes, K., Schmidt, M.W.I., Smernik, R.J., Currie, L.A., Ball, W.P., Nguyen, T.H., Louchouarn, P., Houel, S., Gustafsson, Ö., Elmquist, M., 2007. Comparison of quantification methods to measure fire-derived (black/elemental) carbon in soils and sediments using reference materials from soil, water, sediment and the atmosphere. Glob. Biogeochem. Cycles 21, 355–362.

Holling, C.S., 1973. Resilience and stability of ecological systems. Annu. Rev. Ecol. Syst. 4, 1–23.

Hua, X., Shan, Z., 1996. Pesticide production, usage and its pollution of the environment factor analysis in China. Adv. Environ. Sci. 4, 33–45 (In Chinese).

Jolliffe, I.T., 1986. Principal Component Analysis. Springer-Verlag, Berlin.

Juggins, S., 2017. rioja: Analysis of Quaternary Science Data, R Package Version (0.9–15). http://cran. r-project. org/package= rioja.

Khairy, M.A., Kolb, M., Mostafa, A.R., Elfiky, A., Bahadir, M., 2009. Risk assessment of polycyclic aromatic hydrocarbons in a Mediterranean semi-enclosed basin affected by human activities (Abu Qir Bay, Egypt). J. Hazard. Mater. 170, 389–397.

Khim, J.S., Villeneuve, D.L., Kannan, K., Lee, K.T., Snyder, S.A., Koh, C.H., Giesy, J.P., 1999. Alkylphenols, polycyclic aromatic hydrocarbons, and organochlorines in sediment from Lake Shihwa, Korea: instrumental and bioanalytical characterization. Environ. Toxicol. Chem. 18, 2424–2432.

Kidder, T.R., Zhuang, Y., 2015. Anthropocene archaeology of the yellow river, China, 5000–2000 BP. Holocene 25, 1602–1623.

Leorri, E., Mitra, S., Irabien, M.J., Zimmerman, A.R., Blake, W.H., Cearreta, A., 2014. A 700 year record of combustion-derived pollution in northern Spain: tools to identify the Holocene/Anthropocene transition in coastal environments. Sci. Total Environ. 470–471, 240–247.

Lewis, S.L., Maslin, M.A., 2015. Defining the Anthropocene. Nature 519, 171–180.

Li, X., 2005. Research of Businessman Estate in the Northeast Region in Late Qing. Northeast Normal University, Changchun p. 48 (In Chinese).

Liu, X., Ma, X., 2002. Natural Environmental Changes and Ecological Protection in the Sanjiang Plain. Science press, Beijing (In Chinese).

Liu, W., 1987. The Japanese invaders plundered of coal resources in northeast China in the period of 1905–1945. J. Liaoning Univ. 6, 28–31 (In Chinese).

Lou, Y., Wang, G., Lu, X., Jiang, M., Zhao, K., 2013. Zonation of plant cover and environmental factors in wetlands of the Sanjiang Plain, northeast China. Nordic J. Bot. 31, 748–756.

Luan, Z.Q., Zhang, G.X., Deng, W., Jin-Ming, H.U., Zhou, D.M., 2007. Study on the changes of air temperature and precipitation in the last 50 years in the Sanjiang Plain. J. Arid Land Resour. Environ. 21, 39–43 (In Chinese).

Luo, W., Lu, Y., Giesy, J.P., Wang, T., Shi, Y., Wang, G., Xing, Y., 2007. Effects of land use on concentrations of metals in surface soils and ecological risk around Guanting Reservoir, China. Environ. Geochem. Health 29, 459–471.

Müller, F., Bergmann, M., Dannowski, R., Dippner, J.W., Gnauck, a., Haase, P., Jochimsen, M.C., Kasprzak, P., Kröncke, I., Kümmerlin, R., Küster, M., Lischeid, G., Meesenburg, H., Merz, C., Millat, G., Müller, J., Padisák, J., Schimming, C.G., Schubert, H., Schult, M., Selmeczy, G., Shatwell, T., Stoll, S., Schwabe, M., Soltwedel, T., Straile, D., Theuerkauf, M., 2015. Assessing resilience in long-term ecological data sets. Ecol. Indic. 65, 10–43.

Marques, M., Da, C.M., Mayorga, M.I., Pinheiro, P.R., 2004. Water environments: anthropogenic pressures and ecosystem changes in the Atlantic drainage basins of Brazil. AMBIO: J. Human Environ. 33, 68–77.

Ostroumov, S.A., 2002. Inhibitory analysis of top-down control: new keys to studying eutrophication, algal blooms, and water self-purification. Hydrobiologia 469, 117–129.

Pennisi, E., 2015. Human impacts on ecosystems began thousands of years ago. Science 350, 1452.

Research group on Chinese wetland development and protection, 1998. The historical review of the exploitation in the Sanjiang Plain. Land Nat. Resour. Res. 15–19.

Robbins, J.A., Edgington, D.N., 1975. Determination of recent sedimentation rates in Lake Michigan using Pb-210 and Cs-137. Geochim. Cosmochim. Acta 39, 285–304.

Rosen, A.M., Lee, J., Li, M., Wright, J., Wright, H.T., Fang, H., 2015. The Anthropocene and the landscape of Confucius: a historical ecology of landscape changes in northern and eastern China during the middle to late Holocene. Holocene 25, 75–97.

Ruddiman, W.F., 2003. The Anthropogenic greenhouse era began thousands of years ago. Clim. Change 61, 261–293.

Shu, J., Wang, W., Jiang, L., Takahara, H., 2010. Early Neolithic vegetation history, fire regime and human activity at Kuahuqiao, Lower Yangtze River, East China: new and improved insight. Quat. Int. 227, 10–21.

Smith, F.A., Elliott, S.M., Lyons, S.K., 2010. Methane emissions from extinct megafauna. Nat. Geosci. 3, 374–375.

Song, J., Peng, P., Huang, W., 2002. Black carbon and kerogen in soils and sediments. 1. Quantification and characterization. Environ. Sci. Technol. 36, 3960–3967.

Song, K., Liu, D., Wang, Z., Bai, Z., Cui, J., Fang, L.I., Liu, H., 2008. Land use change in Sanjiang Plain and its driving forces analysis since 1954. Acta Geogr. Sin. 63, 93–104 (In Chinese).

Stankevica, K., Pujate, A., Kalnina, L., Klavins, M., Cerina, A., Drucka, A., Kiziks, K., 2015. Records of the anthropogenic influence on different origin lake sediments of Latvia. Baltica 28, 135–150.

Steffen, W., Crutzen, P.J., McNeill, J.R., 2007. The Anthropocene: are humans now overwhelming the great forces of nature. AMBIO: J. Human Environ. 36, 614–621.

Steffen, W., Grinevald, J., Crutzen, P., Mcneill, J., 2011. The Anthropocene: conceptual and historical perspectives. Philos. Trans. Math. Phys. Eng. Sci. 369, 842.

Steffen, W., Leinfelder, R., Zalasiewicz, J., Waters, C.N., Williams, M., Summerhayes, C., Barnosky, A.D., Cearreta, A., Crutzen, P., Edgeworth, M., 2016. Stratigraphic and earth system approaches to defining the Anthropocene. Earths Future 4, 324–345.

Syvitski, J.P., Kettner, A., 2011. Sediment flux and the Anthropocene. Philos. Trans. 369, 957.

Thomas, C.D., 2015. Rapid acceleration of plant speciation during the Anthropocene. Trends Ecol. Evol. 30, 448–455.

Tian, F., Herzschuh, U., Dallmeyer, A., Xu, Q.H., Mischke, S., Biskaborn, B.K., 2013. Environmental variability in the monsoon-westerlies transition zone during the last 1200 years: lake sediment analyses from central Mongolia and supra-regional synthesis. Quat. Sci. Rev. 73, 31–47.

Vagnetti, R., Miana, P., Fabris, M., Pavoni, B., 2003. Self-purification ability of a resurgence stream. Chemosphere 52, 1781–1795.

Wang, Z.M., Song, K.S., Liu, D.W., Bai, Z., Zhang, S.Q., Fang, L.I., Ren, C.Y., Cui, J., Yang, T., Zhang, C.H., 2009. Process of land conversion from marsh into cropland in the Sanjiang Plain during 1954–2005. Wetland Sci. 7, 208–217 (In Chinese).

Wang, C., Zhao, H., Wang, G., 2015. Vegetation development and water level changes in Shenjiadian peatland in Sanjiang Plain, Northeast China. Chin. Geogr. Sci. 25, 451–461.

Waters, C.N., Zalasiewicz, J., Summerhayes, C., Barnosky, A.D., Poirier, C., Galuszka, A., Cearreta, A., Edgeworth, M., Ellis, E.C., Ellis, M., Jeandel, C., Leinfelder, R., McNeill, J.R., Richter, D.D., Steffen, W., Syvitski, J., Vidas, D., Wagreich, M., Williams, M., An, Z.S., Grinevald, J., Odada, E., Oreskes, N., Wolfe, A.P., 2016. The Anthropocene is functionally and stratigraphically distinct from the Holocene. Science 351 ad2622

aad2622-a-10.
Waters, C.N., 2014. A stratigraphical basis for the Anthropocene? Geol. Soc. Lond. Spec. Publ. 395, 1–21.
White, J.S., Bayley, S.E., 2001. Nutrient retention in a Northern Prairie marsh (Frank Lake, Alberta) receiving municipal and agro-industrial wastewater. Water Air Soil Pollut. 126, 63–81.
Williams, M., Zalasiewicz, J.A., Waters, C.N., Landing, E., 2007. Is the fossil record of complex animal behaviour a stratigraphical analogue for the Anthropocene? Geol. Soc. Lond. Spec. Publi. 10, 459–466.
Williams, M., Zalasiewicz, J., Waters, C.N., Edgeworth, M., Bennett, C., Barnosky, A.D., Ellis, E.C., Ellis, M.A., Cearreta, A., Haff, P.K., do Sul, J.A.I., Leinfelder, R., McNeill, J.R., Odada, E., Oreskes, N., Revkin, A., Richter, D.D., Steffen, W., Summerhayes, C., Syvitski, J.P., Vidas, D., Wagreich, M., Wing, S.L., Wolfe, A.P., An, Z.S., 2016. The Anthropocene: a conspicuous stratigraphical signal of anthropogenic changes in production and consumption across the biosphere. Earths Future 4, 34–53.
Wolfe, A.P., Hobbs, W.O., Birks, H.H., Briner, J.P., Holmgren, S.U., Ingólfsson Ó, Kaushal, S.S., Miller, G.H., Pagani, M., Saros, J.E., 2013. Stratigraphic expressions of the Holocene–Anthropocene transition revealed in sediments from remote lakes. Earth Sci. Rev. 116, 17–34.
Xu, M., Dong, X., Yang, X., Wang, R., Zhang, K., Zhao, Y., Davidson, T.A., Jeppesen, E., 2017. Using palaeolimnological data and historical records to assess long-term dynamics of ecosystem services in typical Yangtze shallow lakes (China). Sci. Total Environ. 584–585, 791–802.
Xue, H., Li, S., 1993. The Comprehensice History of Northeast China. Jilin Cultural and Historical Press, Changchun (In Chinese).
Yang, S.L., Zhao, Q.Y., Belkin, I.M., 2002. Temporal variation in the sediment load of the Yangtze river and the influences of human activities. J. Hydrol. 263, 56–71.
Zalasiewicz, J., Williams, M., Steffen, W., Crutzen, P., 2010. The new world of the Anthropocene. Environ. Sci. Technol. 44, 2228.
Zalasiewicz, J., Waters, C.N., Williams, M., Barnosky, A.D., Cearreta, A., Crutzen, P., Ellis, E., Ellis M. a. Fairchild, I.J., Grinevald, J., Haff, P.K., Hajdas, I., Leinfelder, R., McNeill, J., Odada, E.O., Poirier, C., Richter, D., Steffen, W., Summerhayes, C., Syvitski, J.P.M., Vidas, D., Wagreich, M., Wing, S.L., Wolfe, A.P., An, Z., Oreskes, N., 2015. When did the Anthropocene begin? A mid-twentieth century boundary level is stratigraphically optimal. Quat. Int. 383, 196–203.
Zeileis, A., Leisch, F., Hornik, K., Kleiber, C., 2002. Strucchange: an R package for testing for structural change in linear regression models. J. Stat. Software 7, 1–38.
Zhang, Z., Zhong, J., Lv, X., Tong, S., Wang, G., 2015. Climate, vegetation, and human influences on late-Holocene fire regimes in the Sanjiang Plain northeastern China. Palaeogeogr. Palaeoclimatol. Palaeoecol. 438, 1–8.
Zhuang, Y., Kidder, T.R., 2014. Archaeology of the Anthropocene in the yellow river region, China, 8000–2000 cal. BP. Holocene 24, 1602–1623.